

Trapping, retention and laser cooling of Th^{3+} ions in a multisection linear quadrupole trap

P.V. Borisyyuk, O.S. Vasil'ev, S.P. Derevyashkin, N.N. Kolachevsky, Yu.Yu. Lebedinskii, S.S. Poteshin, A.A. Sysoev, E.V. Tkalya, D.O. Tregubov, V.I. Troyan, K.Yu. Khabarova, V.I. Yudin, V.P. Yakovlev

Abstract. A multisection linear quadrupole trap for Th^{3+} ions is described. Multiply charged ions are obtained by the laser ablation method. The possibility of trapping and retention of $\sim 10^3$ ions is demonstrated in macroscopic time scales of ~ 30 s. Specific features of cooling Th^{3+} ions on the electron transitions with wavelengths of 1088, 690 and 984 nm in Th^{3+} ion are discussed; a principal scheme of a setup for laser cooling is presented.

Keywords: frequency standard, ion trap, thorium, nuclear transition, laser cooling.

1. Introduction

In modern metrology, the international frequency standard is a caesium atomic clock; thus, the present definition of a second is related to the frequency of the radiation corresponding to the electron transition between two sublevels of a hyperfine structure of the fundamental state of the unperturbed ^{133}Cs atom. The best relative error of such a clock reached on a 'caesium fountain' installation is 2×10^{-16} [1]. Impressive achievements of recent years in atomic laser spectroscopy of ultrahigh resolution opened real possibilities for a substantial improvement of the accuracy by several orders of magnitude. Stability and reproducibility of the time/frequency units have been improved as well [2–5]. The incentive to create new-generation high-precision frequency standards is that such a

clock is needed not only for application purposes, but also for fundamental investigations. The latter include problems of the general theory of relativity, which became actual after the detection of gravitation waves [6, 7], and precision determination of fundamental physical constants [8].

The clock accuracy can be enhanced by increasing the frequency of employed atomic oscillators, that is, by substituting a microwave working transition for optical one, in which case the frequency is higher by several orders of magnitude. Nowadays, precision optical clocks are realised on strongly forbidden optical transitions in neutral atoms localised in an optical lattice at a magic wavelength [9–16] and in trapped ions [17–20] which form an ion crystal under cooling to a temperature less than 10^{-5} K. In this case, the record level of the relative inaccuracy was achieved, 1.5×10^{-18} [5]. However, further progress encountered a series of principal physical limitations issuing from the sensitivity of the electron subsystem of atoms to external electromagnetic factors, which results in systematic frequency shifts with differing characteristics. Thus, for reaching the level of the relative frequency error of less than 10^{-19} , new approaches should be developed.

Presently, one of the most promising approaches capable of attaining the mentioned error level is the employment of a unique transition in the even–odd thorium-229 nucleus. The thorium nucleus has an isomeric state with the excitation energy comparable to the energies of optical photons and valence electrons. Since the nucleus polarisability is very small and is shielded by the electron shell, nuclear transitions are substantially less sensitive to external perturbations, i.e. electric fields, collisions, etc. The employment of such nuclear transitions gives a principal possibility to improve the measurement accuracy by several orders of magnitude [21–24]. In addition, the transition wavelength in the thorium nucleus is in the near-UV range, which opens the possibility of its use in practice as a standard reference of time and frequency with the employment of femtosecond combs [25, 26]. It can also be used for developing new optical devices operating in the VUV range [27].

Thorium-229 is produced in alpha decay of uranium-233 (^{233}U) with a half-life of 7880 years [28]. In first studies [29] of ^{229}Th nucleus energy levels using the methods of gamma-spectroscopy it was found that the head levels of two rotational bands (the ground and isomeric) are very close to each other. In [30], the energy difference between them was estimated as 1 ± 4 eV, and in [31] – as 3.5 ± 1.0 eV. Further investigations gave an estimate for the value of the nuclear matrix element of the transition between the ground and isomeric states for the ^{229}Th nucleus [24, 32], and an insight into the decay channels for the low-energy level of isomer in an isolated atom (internal conversion and electronic bridge [33], α -decay [34]), in a metal

P.V. Borisyyuk, O.S. Vasil'ev, S.P. Derevyashkin, Yu.Yu. Lebedinskii, S.S. Poteshin, A.A. Sysoev, V.I. Troyan, V.P. Yakovlev National Research Nuclear University 'MEPhI', Kashirskoe sh. 31, 115409 Moscow, Russia; e-mail: pvborisyuk@mephi.ru;
N.N. Kolachevsky, D.O. Tregubov National Research Nuclear University 'MEPhI', Kashirskoe sh. 31, 115409 Moscow, Russia;
 P.N. Lebedev Physical Institute, Russian Academy of Sciences, Leninsky prosp. 53, 119991 Moscow, Russia; Moscow Institute of Physics and Technology (State University), Institutskii per. 9, 141700 Dolgoprudnyi, Moscow region, Russia; e-mail: treg.dim@gmail.com;
E.V. Tkalya National Research Nuclear University 'MEPhI', Kashirskoe sh. 31, 115409 Moscow, Russia; D.V. Skobel'tsyn Institute of Nuclear Physics, M.V. Lomonosov Moscow State University, Vorob'evy gory, 119991 Moscow, Russia; Nuclear Safety Institute, Russian Academy of Sciences, Bol'shaya Tul'skaya ul. 52, 115191 Moscow, Russia; e-mail: tkalya@srd.sinp.msu.ru;
K.Yu. Khabarova P.N. Lebedev Physical Institute, Russian Academy of Sciences, Leninsky prosp. 53, 119991 Moscow, Russia; Moscow Institute of Physics and Technology (State University), Institutskii per. 9, 141700 Dolgoprudnyi, Moscow region, Russia;
V.I. Yudin Novosibirsk State University, ul. Pirogova 2, 630090 Novosibirsk, Russia; e-mail: viyudin@mail.ru

Received 9 March 2017

Kvantovaya Elektronika 47 (5) 406–411 (2017)

Translated by N.A. Raspopov

(inelastic scattering of conduction electrons on isomer nuclei [35]) and in a dielectric crystal with a wide forbidden band ('nuclear light' [36, 37]). A lifetime of this level for different decay channels was estimated in [24, 33, 34, 37]. In particular, in a crystal with a wide forbidden band, the lifetime of the isomeric state of the ^{229}Th nucleus may be 10^3 – 10^4 s [24]. Note that in recent experiment [38], the measured lifetime of the excited state of the neutral atom in the decay by the electron conversion channel is 7 ± 1 μs . This value is close to the theoretical estimate of 10 μs given in [24], in reasonable agreement with the very first estimate of 2 μs made in 1991 [33].

Presently, the best experimental results on optical spectroscopy of quantum states of ion ensembles of thorium-229 localised in a radio frequency trap have been obtained by two research groups in the USA and Germany. In Germany, the laser systems for spectroscopy of electron transitions in thorium and the ion trap for obtaining an ensemble of Th^{3+} ions were developed. Spectra of quantum states of thorium were investigated and the corresponding fine structure was studied [39–41]. In the USA, the laser systems for spectroscopy of electron transitions in thorium and the ion trap for Th ions were created. Laser cooling of ion Th^{3+} ions was performed; first Th^{3+} coulomb crystals, which include up to 10^4 ions, have been obtained and investigated [42]. The budget of errors was estimated for the standard on a nuclear transition in thorium [22]. With the allowance made for the quadratic and linear Zeeman effects, Stark effect, linear Doppler effect, blackbody radiation, the influence of gravitational field and micro-motion of the ion in the trap, the total uncertainty of the clock amounts to 10^{-19} and may probably reach 10^{-20} .

Laser cooling of a thorium ion ensemble in a trap for spectroscopy investigations of a nuclear isomeric transition is technically difficult, but the main problem is to excite the isomeric transition in Th nucleus. Recall that direct excitation of the transition has not been realised yet because of the large uncertainty in the value of the transition energy and a long lifetime of the excited state. Hence, it seems realistic to excite the isomeric level by using the mechanism of an inverse electronic bridge, which was first suggested in [43, 44] (see also [45]) for the thulium atom and then generalised to the case of the Th^+ ion [46]. This mechanism in the case of the favourable level configuration (namely, at a small difference between the energies of the nuclear transition and one of the atomic magneto-dipole transitions) has a substantially greater cross section than the process of direct photo-excitation; in addition, it implies adjustment of the laser radiation frequency to the frequencies of well-known and relatively broadband atomic transitions.

Thus, one may state that intensive efforts of experimenters on measuring the frequency of the low-level isomeric transition in the thorium-229 nucleus made for last years in a number of leading scientific centres have not yielded the desired result. Nevertheless, this is an important step towards the creation of the precise frequency standard on ultra-cold ions $^{229}\text{Th}^{3+}$. In the present work, we present the results of our experimental investigations related to obtaining $^{229}\text{Th}^{3+}$ ions and trapping them in an original trap with the aim of further laser cooling.

2. Production of multiply charged thorium ions

Even the first step, namely, obtaining thorium in the atomic state is a challenging problem, because thorium is a refractory metal with a high melting temperature of 2023 K [47]

and low saturation vapour pressure. In addition, due to high reactivity, thorium easily forms the ThO_2 oxide, which possesses melting temperatures of ~ 3000 K [47]. In experiments on laser cooling and spectroscopy of thorium quantum states, Th^{3+} [48] and Th^+ [49] ions are used. Since the triply charged Th^{3+} ion with one valence electron has a simpler system of electron levels than lower-charge ions (Th^{2+} , Th^+), this ion is preferable for precision spectroscopic investigations of the low-lying isotopic nuclear transition. The direct detection of such a transition is related to the process of emitting a γ -quantum in spontaneous relaxation of the nucleus isomeric state. Two complicated systems of overlapping electron levels in the ground and isomeric thorium states can substantially increase (through the electronic bridge mechanism) the probability of other relaxation channels for the metastable nucleus state while exciting the electron system; thus, this can disguise the process of emitting a high-energy photon.

In our experiments, triply charged thorium ions were obtained by the laser ablation method. Because of the high radioactivity of the ^{229}Th isotope, at the initial stage of the experiment we used a sample of mono-isotopic and chemically inert bulk gold ^{197}Au and stable isotope ^{232}Th .

During the ablation process a short laser pulse generates a plasma plume with the number of particles $\sim 10^{13}$ [50], which allows one to trap a great number of ions. The method of laser ablation provides local evaporation of a target [51], which is ideally suited for working with a limited quantity of material. It is important, because the maximal admissible activity of a sample in laboratory conditions is 1 kBq, which corresponds to 10^{14} atoms of ^{229}Th , or subnanogram of substance.

The system for obtaining thorium ions by laser ablation is realised on a flashlamp-pumped, Q -switched Nd:YAG laser with the following parameters: the laser pulse duration is 25 ns, pulse energy is 560 mJ, and radius of the focused laser spot on a sample is 100 μm . The radiation intensity on a sample was 7.4 GW cm^{-2} . Characteristics of the ion beam were measured by using the time-of-flight mass-spectrometry technique. Ions were detected at a distance of 0.5 m by a VEU-6M secondary electron multiplier (SEM), in front of which an energy analyser was placed for filtering of detected ions with respect to energy.

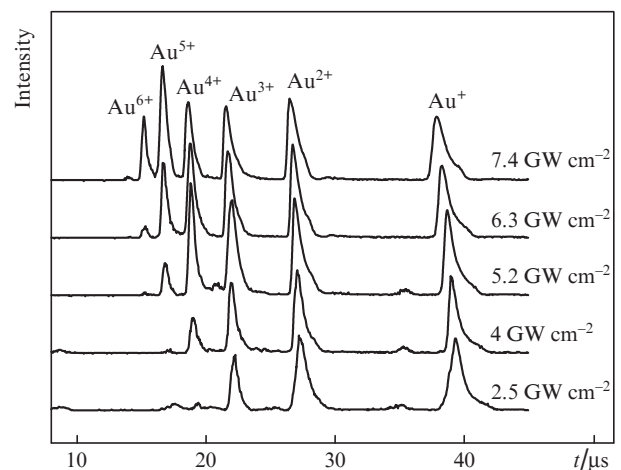


Figure 1. Time-of-flight mass spectra of gold at various intensities of laser radiation on the sample.

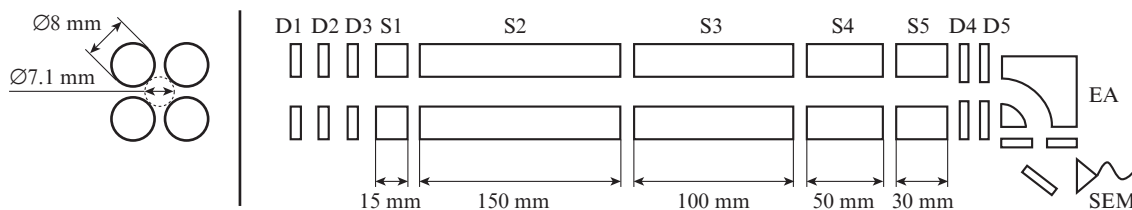


Figure 2. Scheme of a multisection quadrupole ion trap: (D1–D5) diaphragms; (S1–S5) trap sections; (EA) energy analyser; (SEM) secondary electron multiplier. The transverse cross section of quadrupole rods is shown on the left side.

Time-of-flight mass-spectra of gold ions measured at various intensities of laser radiation on a sample are presented in Fig. 1. The energy analyser was adjusted to transmit the ions with the energy of 150 eV at the transmission bandwidth of 50 eV. At $t = 39 \mu\text{s}$, the peak corresponding to the time-of-flight for Au^+ is observed; Au^{2+} , Au^{3+} , Au^{4+} , Au^{5+} and Au^{6+} ions are responsible for the peaks at instants 27, 22, 19, 17 and 15 μs , respectively. With increasing radiation intensity on a sample, the peaks, corresponding to a higher ion charge, arise. At intensities of $\sim 10 \text{ GW cm}^{-2}$, gold ions with the charge multiplicity of up to 6+ are generated, which corresponds to results obtained in [52].

3. Capturing ions in a quadrupole trap with linear configuration

Spectroscopy investigations of thorium quantum states necessitate ion trapping and retention for an extended time. An original multisection quadrupole ion trap with the linear configuration was used [53], which comprised five independent successive quadrupole segments separated by silica insulators (Fig. 2). A quadrupole-based trap can be made extremely compact [54].

The trap rods are supplied with the oscillating voltage U_{rf} of the amplitude 338 V and a frequency of 1.22 MHz. An additional constant voltage $U_{\text{dc}} \leq 400 \text{ V}$ can be applied to section S2 of length 150 mm. A proper choice of the voltage amplitudes U_{rf} and U_{dc} provides radial retention of ions and mass filtering in the range of 2–250 a.e.m. with a resolution of 1 a.e.m. As noted, detected ions were filtered with respect to energy by means of an energy analyser placed in front of the secondary electron multiplier.

Diaphragms D3 and D4 with the holes of diameter 5 mm, coaxial to the trap axis, are placed on the end faces of the trap. Ion trapping is realised by applying to the diaphragms the ‘trapping’ potentials of $\sim 100 \text{ V}$ synchronously with the laser pulse (with the synchronisation accuracy of 1 μs), which provides ion trapping in the direction of the trap axis.

Independent sections in the trap allow one to vary the potential at the axis of each quadrupole, and to form a potential profile that may change in time. Thus, it is possible to use a multistage mechanism of ion trapping and gradually localise ions in a progressively smaller space volume. The employment of the multistage process of ion trapping increases the trapping efficiency by an order of magnitude and more [53]. In addition, by applying a positive potential simultaneously to all sections of the trap it is possible to change the kinetic energy of ions, slowing them down prior to entering the trapping zone and, thus, to attain the maximum of ion distribution over energy. At the intensity of laser radiation used in ablation, this maximum is near 150 eV. Trapping of ions, which possess the energy corresponding to the maximum of

the energy distribution, substantially increases the number of trapped ions. This feature allows one to trap the ions with the initial kinetic energy of 1–500 eV.

Figure 3 shows see an oscillogram from the SEM, which demonstrates the process of ion trapping with the retention time of $\sim 30 \text{ s}$.

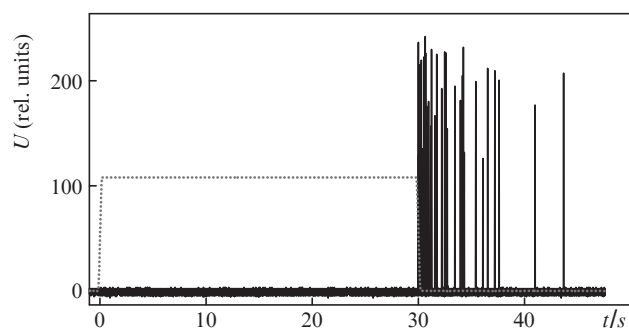


Figure 3. Oscillogram of a SEM signal (solid curve), illustrating the process of ion trapping; dashed line shows the blanking voltage applied to the diaphragms. Instant of the laser pulse onset is taken as a zero time point.

The SEM signal, which is observed after switching off the blanking voltage, demonstrates the possibility of retaining ions for macroscopic time $\sim 30 \text{ s}$. The number of detected ions is ~ 50 , which, taking into account high losses in the energy analyser ($\sim 10^{-2}$), gives an estimate for trapped ions at a level of 10^3 .

4. Energy level diagrams of $^{232}\text{Th}^{3+}$ and $^{229}\text{Th}^{3+}$ ions

For successful Doppler cooling of ions it is necessary to know the structure of the energy levels of the ion and the parameters of transitions between the levels. The energy level diagrams for $^{232}\text{Th}^{3+}$ and $^{229}\text{Th}^{3+}$ ions are shown in Fig. 4.

The electron levels of the $^{232}\text{Th}^{3+}$ isotope have no hyperfine structure (Fig. 4a), because the nuclear spin of this isotope is zero. The wavelength of the $5F_{5/2} \rightarrow 6D_{3/2}$ transition is 1088 nm, and the natural linewidth γ of the upper level $6D_{3/2}$ is 145 kHz, according to [55]. The level $6D_{5/2}$ has the natural linewidth $\gamma = 234 \text{ kHz}$ and decays with the branching factor 1:8 into the two sublevels, $5F_{5/2}$ and $5F_{7/2}$, of the hyperfine structure of the ground state. The wavelengths of the corresponding transitions are 690 and 984 nm.

In contrast to $^{232}\text{Th}^{3+}$, the spin of the $^{229}\text{Th}^{3+}$ isotope is distinct from zero ($I = 5/2$), which makes its hyperfine structure rather complicated. A variety of transitions in the $^{229}\text{Th}^{3+}$ ion can be described by the formula [56]

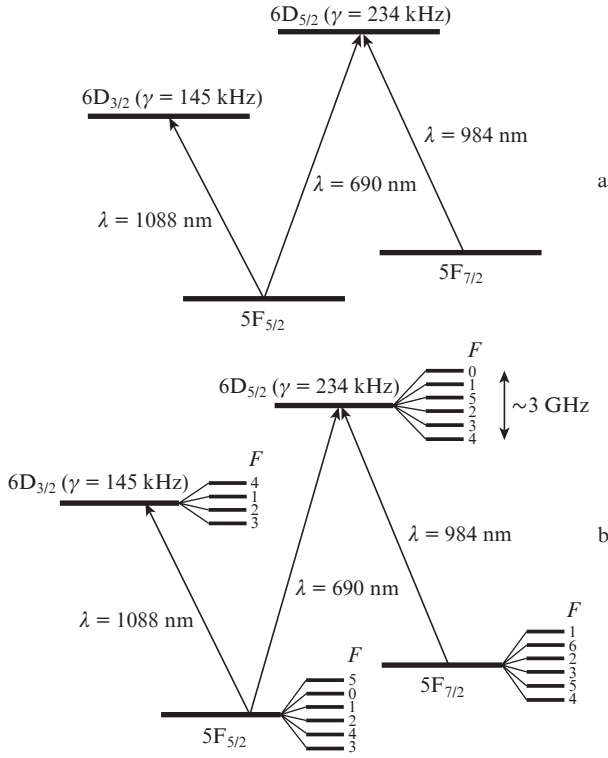


Figure 4. Energy levels of (a) ²³²Th³⁺ and (b) ²²⁹Th³⁺ ions used for cooling.

$$\delta E_{c,g} = \frac{K_e}{2} A_e + \frac{3K_e(K_e + 1)/2 - 2I(I + 1)J_e(J_e + 1)}{4I(2I - 1)J_e(2J_e - 1)} B_e - \frac{K_g}{2} A_g - \frac{3K_g(K_g + 1)/2 - 2I(I + 1)J_g(J_g + 1)}{4I(2I - 1)J_g(2J_g - 1)} B_g + \Delta, \quad (1)$$

where $\delta E_{c,g}$ is the energy difference between the corresponding transitions in the ²²⁹Th³⁺ and ²³²Th³⁺ ions; $K_i = F_i(F_i + 1) - I(I + 1) - J_i(J_i + 1)$; I is the nuclear spin; J is the total momentum of the electron shell; F_i is the total atomic momentum; $i = g(e)$ (subscripts g and e correspond to the ground and excited electron levels); A is the magnetic dipole coefficient; B is the electric quadrupole coefficient; and Δ is the isotopic shift common for all hyperfine components of a particular level. Coefficients A , B and Δ for all three transitions were measured in [48].

5. Doppler cooling

A simpler structure of ²³²Th³⁺ isotope levels substantially facilitates the procedure of laser cooling for these ions. The closed transition with $\lambda = 1088$ nm is convenient for Doppler cooling. As for the transitions with $\lambda = 690$ nm and $\lambda = 984$ nm, these form a closed three-level system with the preferable (as 8 : 1) spontaneous decay through the right channel (see Fig. 4a). Hence, for the optimal Doppler cooling, one may vary the radiation frequency detuning from the transition 984 nm, while using the transition 690 nm only for repumping purposes.

A rich hyperfine structure of the ²²⁹Th³⁺ isotope complicates the process. The ground ($5F_{5/2}$) and excited ($6D_{3/2}$) levels of the transition with $\lambda = 1088$ nm split to 6 and 4 components, respectively. In the process of cooling, the decay of the excited electron state of the ²²⁹Th³⁺ ion from a particular hyperfine sublevel F may occur to sublevels F , $F \pm 1$ of the

ground state. Hence, there is no ‘ideal’ two-level scheme, and it is necessary to excite a number of transitions (Fig. 5) in order to prevent the origin of ‘dark’ states, fitting to which the ion leaves the cooling cycle. A fine adjustment of the radiation frequency in this case becomes a nontrivial task, and cooling on the transition with $\lambda = 1088$ nm can only be used as the first cooling stage (primary cooling) for attaining temperatures of ~ 10 K. At such temperatures, the Doppler broadening is sufficiently small (~ 200 MHz) and does not prevent further cooling at the second stage (secondary cooling).

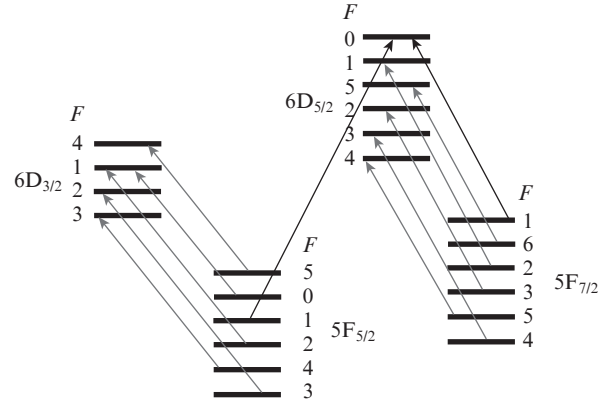


Figure 5. Schematic of Doppler cooling for the ²²⁹Th³⁺ ion.

The second cooling stage occurs on the transitions with $\lambda = 690$ nm and $\lambda = 984$ nm. Similarly to the case of the ²³²Th³⁺ ion, for ²²⁹Th³⁺ there is a closed three-level scheme $5F_{5/2}(F = 1) \leftrightarrow 5D_{5/2}(F = 0) \leftrightarrow 5F_{7/2}(F = 1)$ (the transition $F = 0 \rightarrow F = 0$ is forbidden by the selection rules). In this case, adjustment of the radiation frequency is much simpler, because only one transition is excited between hyperfine sublevels. Although the transition to another sublevel $5D_{5/2}(F = 1)$ is offset by ~ 600 MHz, there is a probability of the non-resonance excitation of transitions beyond the three-level scheme; hence, repumping lasers are needed (Fig. 5).

For efficient operation of the secondary cooling it is necessary that in the process of primary cooling the radiation at $\lambda = 1088$ nm pumps ions to the sublevel $5F_{5/2}(F = 1)$ as well. It is realised by choosing the appropriate cooling transitions, for which $5F_{5/2}(F = 1)$ becomes the ‘dark’ state for the primary cooling (Fig. 5).

At a first stage of the experiment, it is interesting to use the so-called sympathetic cooling of ²²⁹Th³⁺ ions by ²³²Th³⁺ ions [48]. This approach is simpler than the direct cooling because of the missing hyperfine structure in ²³²Th³⁺ ions.

6. Systems of laser cooling and detection

Since the isotopic frequency shifts of all three described transitions are ~ 10 GHz, ions of both isotopes can be cooled with the same lasers by tuning their frequencies prior to conducting an experiment. In addition, it may be done simultaneously by using the ± 1 harmonics of an electro-optical phase modulator (EOPM). Such a modulator is also needed for exciting a series of cooling transitions between hyperfine components of the ²²⁹Th³⁺ ion.

A scheme of the installation suggested for cooling ions and their detection is presented in Fig. 6. For exciting all the three transitions, we plan to use commercial external-cavity

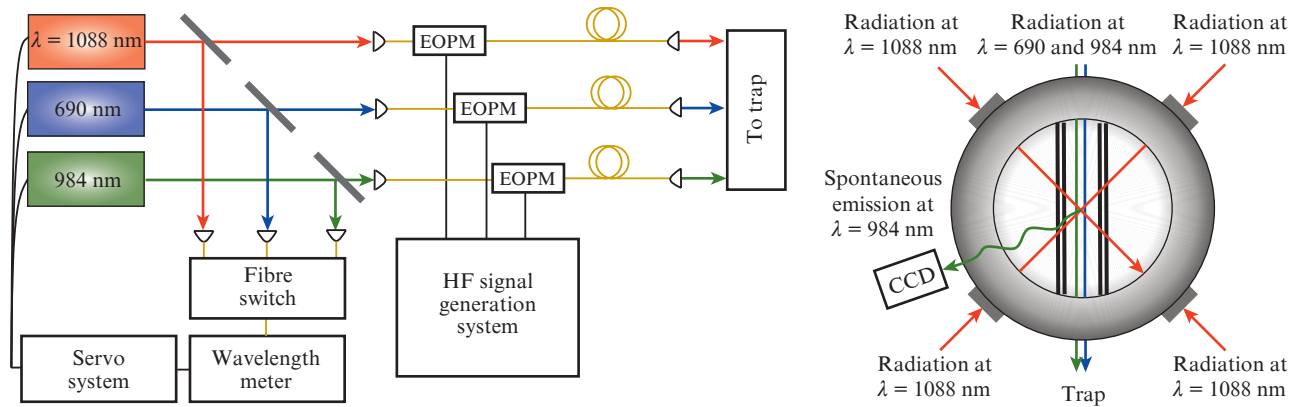


Figure 6. Schematic of the installation for Doppler cooling of Th^{3+} ions.

diode lasers. The range of continuous tuning of their frequencies is 20 GHz and covers the isotopic shift, as well as all intervals of hyperfine splitting, which simplifies the experiment with two isotopes involved. We suggest stabilising the frequency of laser radiation at the first stage by a wavelength meter. This method is capable of stabilising the frequency at a level of several MHz, which is not sufficient for deep cooling on a transition with the natural linewidth of about 200 kHz. Further, we plan to stabilise the laser radiation frequency by the Pound–Drever–Hall stabilisation method [57].

It is reasonable to use one of the transitions involved in cooling for optical detection of ions. Only one of these transitions, which has $\lambda = 690$ nm, is in the visible spectral range. However, this decay channel has a small branching factor, and more attractive for the detection system seems the transition at $\lambda = 984$ nm. Although it is beyond the visible spectral range, there are CCDs operating in this spectral range.

7. Excitation of the nuclear transition of ^{229}Th in the trap

Since the laser radiation and electron beam are available, there are three simplest and natural methods for exciting ^{229}Th nuclei to the low state $3/2^+(7.8 \pm 0.5$ eV): it is the inelastic electron scattering on thorium-229 ions, excitation by the laser radiation according to the inverse electronic bridge mechanism [43–46], and direct photoexcitation of nuclei [23, 44, 45]. Unfortunately, the position of the nuclear isomeric level relative to the energy spectrum of electron states of $^{229}\text{Th}^{1+,3+}$ ions is not actually known yet. Thus, the potentially most efficient excitation mechanism through the electronic bridge may be useless due to a very large mismatch between the frequencies of the nuclear and electron transitions. In this case, either an electron beam should be used, or the laser radiation frequency should be exactly (within the laser line bandwidth) matched with the frequency of the nuclear transition. The latter may be hardly realised technically. Excitation by an electron beam has a simple advantage that all electrons having the energy above the nuclear isomer energy level will participate in the reaction. Hence, the choice of a particular method for obtaining isomeric nuclei in a Paul trap will depend on results of further investigations on determining the energy of the nuclear state $3/2^+(7.8 \pm 0.5$ eV).

Thus, we have demonstrated operation of a multisection linear quadrupole trap for capturing and retention of Th^{3+} ions. The ions were produced by laser ablation, which allows one to trap a large number of ions at small material expendi-

ture. A scheme of laser cooling for Th^{3+} ions is described, and a schematic diagram of the installation is presented.

Acknowledgements. The authors are grateful to A.V. Zenkevich and Yu.N. Kolosov for the help in conducting experiments and discussing the results.

The work was supported by the Russian Science Foundation (Pproject No. 16-12-00001).

References

- Levi F., Calonico D., Calosso C.E., Godone A., Micalizio S., Costanzo G.A. *Metrologia*, **51** (3), 270 (2014).
- Ludlow A.D., Boyd M.M., Ye J., Peik E., Schmidt P.O. *Rev. Modern Phys.*, **87**, 637 (2015).
- Taichenachev A.V., Yudin V.I., Bagayev S.N. *Phys. Usp.*, **186**, 193 (2016) [*Usp. Fiz. Nauk*, **186**, 193 (2016)].
- Riehle F. *Frequency Standards: Basic and Applications* (New York: Wiley, 2004; Moscow: Fizmatlit, 2009).
- Schioppo M., Brown R.C., McGrew W.F., Hinkley N., Fasano R.J., Bely K., Yoon T.H., Milani G., Nicolodi D., Sherman J.A., Phillips N.B. *Nat. Photonics*, **11**, 48 (2017).
- Abbott B.P., Abbott R., Abbott T.D., Abernathy M.R., Acernese F., Ackley K., Adams C., Adams T., Addesso P., Adhikari R.X., Adya V.B. *Phys. Rev. Lett.*, **116**, 061102 (2016).
- Flambaum V. *Phys. Rev. Lett.*, **117**, 072501 (2016).
- Flambaum V. *Phys. Rev. Lett.*, **97**, 092502 (2006).
- Ushijima I., Takamoto M., Das M., Ohkubo T., Katori H. *Nat. Photonics*, **9**, 185 (2015).
- Nicholson T.L., Campbell S.L., Hutson R.B., Marti G.E., Bloom B.J., McNally R.L., Zhang W., Barrett M.D., Safronova M.S., Strouse G.F., Tew W.L. *Nat. Commun.*, **6**, 6896 (2015).
- Hinkley N., Sherman J.A., Phillips N.B., Schioppo M., Lemke N.D., Bely K., Pizzocaro M., Oates C.W., Ludlow A.D. *Science*, **341**, 1215 (2013).
- Le Targat R., Lorini L., Le Coq Y., Zawada M., Guéna J., Abgrall M., Gurov M., Rosenbusch P., Rovera D.G., Nagórny B., Gartman R. *Nat. Commun.*, **4**, 2109 (2013).
- Bloom B.J., Nicholson T.L., Williams J.R., Campbell S.L., Bishof M., Zhang X., Zhang W., Bromley S.L., Ye J. *Nature*, **506**, 71 (2014).
- Bely K., Hinkley N., Phillips N.B., Sherman J.A., Schioppo M., Lehman J., Feldman A., Hanssen L.M., Oates C.W., Ludlow A.D. *Phys. Rev. Lett.*, **113**, 260801 (2014).
- Falke S., Lemke N., Grebing C., Lipphardt B., Weyers S., Gerginov V., Huntemann N., Hagemann C., Al-Masoudi A., Häfner S., Vogt S. *New J. Phys.*, **16**, 073023 (2014).
- Kulosa A.P., Fim D., Zipfel K.H., Rühmann S., Sauer S., Jha N., Gibble K., Ertmer W., Rasel E.M., Safronova M.S., Safronova U.I. *Phys. Rev. Lett.*, **115**, 240801 (2015).
- Huntemann N., Sanner C., Lipphardt B., Tamm C., Peik E. *Phys. Rev. Lett.*, **116**, 063001 (2016).

18. Chou C., Hume D., Koelemeij J., Wineland D., Rosenband T. *Phys. Rev. Lett.*, **104**, 070802 (2010).
19. Madej A.A., Dubé P., Zhou Z., Bernard J.E., Gertsvolf M. *Phys. Rev. Lett.*, **109**, 203002 (2012).
20. Godun R.M., Nisbet-Jones P.B., Jones J.M., King S.A., Johnson L.A., Margolis H.S., Szymaniec K., Lea S.N., Bongs K., Gill P. *Phys. Rev. Lett.*, **113**, 210801 (2014).
21. Peik E., Tamm C. *Europhys. Lett.*, **61**, 181 (2003).
22. Campbell C.J., Radnaev A.G., Kuzmich A., Dzuba V.A., Flambaum V.V., Derevianko A. *Phys. Rev. Lett.*, **108**, 120802 (2012).
23. Yamaguchi A., Kolbe M., Kaser H., Reichel T., Gottwald A., Peik E. *New J. Phys.*, **17**, 053053 (2015).
24. Tkalya E., Schneider C., Jeet J., Hudson E.R. *Phys. Rev. C*, **92**, 054324 (2015).
25. Von der Wense L., Seiferle B., Laatiaoui M., Neumayr J.B., Maier H.J., Wirth H.F., Mokry C., Runke J., Eberhardt K., Düllmann C.E., Trautmann N.G. *Nature*, **533**, 47 (2016).
26. Peik E., Okhapkin M. *Compt. Rend. Phys.*, **16**, 516 (2015).
27. Tkalya E. *Phys. Rev. Lett.*, **106**, 162501 (2011).
28. Browne E., Tuli J. *Nucl. Data Sheets*, **109**, 2657 (2008).
29. Kroger L., Reich C. *Nucl. Phys. A*, **259**, 29 (1976).
30. Reich C., Helmer R. *Phys. Rev. Lett.*, **64**, 271 (1990).
31. Helmer R., Reich C. *Phys. Rev. C*, **49**, 1845 (1994).
32. Dykhne A., Tkalya E. *Pis'ma Zh. Eksp. Teor. Fiz.*, **64**, 521 (1998).
33. Strizhov V., Tkalya E. *Zh. Eksp. Teor. Fiz.*, **99**, 697 (1991).
34. Dykhne A., Eremin N., Tkalya E. *Pis'ma Zh. Eksp. Teor. Fiz.*, **64**, 319 (1996).
35. Tkalya E. *Pis'ma Zh. Eksp. Teor. Fiz.*, **70**, 367 (1999).
36. Tkalya E. *Pis'ma Zh. Eksp. Teor. Fiz.*, **71**, 449 (2000).
37. Tkalya E.V., Zherikhin A.N., Zhudov V.I. *Phys. Rev. C*, **61**, 064308 (2000).
38. Seiferle B., von der Wense L., Thirof P.G. *Phys. Rev. Lett.*, **118**, 042501 (2017).
39. Herrera-Sancho O., Nemitz N., Okhapkin M., Peik E. *Phys. Rev. A*, **88**, 012512 (2013).
40. Herrera-Sancho O.A., Okhapkin M.V., Zimmermann K., Tamm C., Peik E., Taichenachev A.V., Yudin V.I., Głowacki P. *Phys. Rev. A*, **85**, 033402 (2012).
41. Okhapkin M.V., Meier D.M., Peik E., Safronova M.S., Kozlov M.G., Porsev S.G. *Phys. Rev. A*, **92**, 020503 (2015).
42. Radnaev A., Campbell C., Kuzmich A. *Phys. Rev. A*, **86**, 060501 (2012).
43. Tkalya E. *Pis'ma Zh. Eksp. Teor. Fiz.*, **55**, 216 (1992).
44. Tkalya E. *Yad. Fiz.*, **55**, 2881 (1992).
45. Tkalya E., Varlamov V., Lomonosov V., Nikulin S. *Phys. Scripta*, **53**, 296 (1996).
46. Porsev S., Flambaum V., Peik E., Tamm C. *Phys. Rev. Lett.*, **105**, 182501 (2010).
47. Grigoriev I.S., Melikhov E.Z. (Eds) *Handbook of Physical Quantities* (Boca Raton: CRC Press, 1997; Moscow: Energoatomizdat, 1991).
48. Campbell C., Radnaev A., Kuzmich A. *Phys. Rev. Lett.*, **106**, 223001 (2011).
49. Zimmermann K., Okhapkin M., Herrera-Sancho O., Peik E. *Appl. Phys. B*, **107**, 883 (2012).
50. Borman V.D., Zenkevich A.V., Nevolin V.N., Pushkin M.A., Tronin V.N., Troyan V.I. *Zh. Eksp. Teor. Fiz.*, **130**, 984 (2006).
51. Troyan V.I., Borisjuk P.V., Khalitov R.R., Krasavin A.V., Lebedinskii Y.Y., Palchikov V.G., Poteshin S.S., Sysoev A.A., Yakovlev V.P. *Laser Phys. Lett.*, **10**, 105301 (2013).
52. Torrisi L., Picciotto A., Ando L., Gammino S., Margarone D., Láská L., Pfeifer M., Krása J. *Czechosl. J. Phys.*, **54**, 421 (2004).
53. Troyan V.I., Borisjuk P.V., Krasavin A.V., Vasiliev O.S., Palchikov V.G., Avdeev I.A., Chernyshev D.M., Poteshin S.S., Sysoev A.A. *Europ. J. Mass Spectrom.*, **21**, 1 (2015).
54. Ketola R.A., Kiuru J.T., Tarkiainen V., Kotiaho T., Sysoev A.A. *Rapid Commun. Mass Spectrom.*, **17**, 753 (2003).
55. Safronova U.I., Johnson W.R., Safronova M.S. *Phys. Rev. A*, **74**, 042511 (2006).
56. Sobelman I.I. *Introduction to the Theory of Atomic Spectra* (Oxford: Pergamon Press, 1979; Moscow: Fizmatlit, 1963).
57. Black E.D. *Am. J. Phys.*, **69**, 79 (2001).